Molecular and Cellular Biochemistry **229:** 163–171, 2002.

Short communication

Inhibitory effects of extracellular Mg^{2+} on intracellular Ca^{2+} dynamic changes and thapsigargin-induced apoptosis in human cancer MCF7 cells

Manuella Pereira,[1] Jean-Marc Millot,[1] Stephane Sebille[2] and Michel Manfait[1]

[1]*Unité MéDIAN, CNRS FRE 2141, Faculté de Pharmacie, Reims Cedex;* [2]*Laboratoire de Biomembrane et Signalisation Cellulaire, Faculté des Sciences, Poitiers, France*

Received 25 May 2001; accepted 19 October 2001

Abstract

The effects of extracellular Mg^{2+} on both dynamic changes of $[Ca^{2+}]_i$ and apoptosis rate were analysed. The consequences of spatial and temporal dynamic changes of intracellular Ca^{2+} on apoptosis, in thapsigargin- and the calcium-ionophore 4BrA23187-treated MCF7 cells were first determined. Both 4BrA23187 and thapsigargin induced an instant increase of intracellular Ca^{2+} concentrations ($[Ca^{2+}]_i$) which remained quite elevated (> 150 nM) and lasted for several hours. $[Ca^{2+}]_i$ increases were equivalent in the cytosol and the nucleus. The treatments that induced apoptosis in MCF7 cells were systematically associated with high and sustained $[Ca^{2+}]_i$ (150 nM) for several hours. The initial $[Ca^{2+}]_i$ increase was not determinant in the events triggering apoptosis. Thapsigargin-mediated apoptosis and $[Ca^{2+}]_i$ rise were abrogated when cells were pretreated with the calcium chelator BAPTA. The role of the extracellular Mg^{2+} concentration has been studied in thapsigargin treated cells. High (10 mM) extracellular Mg^{2+}, caused an increase in basal $[Mg^{2+}]_i$ from 0.8 ± 0.3 to 1.6 ± 0.5 mM. As compared to 1.4 mM extracellular Mg^{2+}, 1 μM thapsigargin induces, in 10 mM Mg^{2+}, a reduced percentage from 22 to 11% of fragmented nuclei, a lower sustained $[Ca^{2+}]_i$ and a lower Ca^{2+} influx through the plasma membrane. In conclusion, the cell death induced by thapsigargin was dependent on high and sustained $[Ca^{2+}]_i$ which was inhibited by high extracellular and intracellular Mg^{2+}. (Mol Cell Biochem **229**: 163–171, 2002)

Key words: Ca^{2+}, Mg^{2+}, apoptosis, MCF7 cells

Introduction

Apoptosis or programmed cell death is an active cellular process characterized by distinctive morphological changes that include reduction in nuclear size, condensation of nuclear chromatin, cell shrinkage, disruption of the cytoskeleton, and plasma membrane blebbing [1]. The molecular hallmark of apoptosis is the degradation of cell nuclear DNA into oligonucleosome fragments, as the result of an activation of endogenous endonucleases [2]. This phenomenon seems further to be a highly regulated process of cell deletion involved in the proper development and homeostasis of many tissues [3, 4].

Earlier studies have revealed that free Ca^{2+} could be involved in apoptosis either by changes in the cytosolic Ca^{2+} concentrations ($[Ca^{2+}]_i$) and/or intracellular Ca^{2+} compartmentalization [5, 6]. Experiments on nuclei isolated from thymocytes clearly demonstrated the induction of a Ca^{2+}-

Address for offprints: J.-M. Millot, Unité MéDIAN, CNRS FRE 2141, Faculté de Pharmacie, 51 rue Cognacq-Jay, 51096 Reims Cedex, France (E-mail: jm.millot@univ-reims.fr)

dependent endonuclease activity during triggering apoptosis events [7]. A nuclear Ca^{2+}/Mg^{2+} dependent endonuclease, which is able to digest chromatin *in situ* into mono- and oligonucleosomal fragments, has been purified from human spleen cells [8]. Rises in $[Ca^{2+}]_i$ were then believed to activate this nuclease and to mediate DNA cleavages into oligonucleosome fragments.

At the cell level, sustained $[Ca^{2+}]_i$ increases have been frequently reported in cells induced to undergo apoptosis [9, 10]. Chemical toxins or radiations can promote apoptosis and concomitantly disrupt intracellular Ca^{2+} homeostasis, leading to non-physiological $[Ca^{2+}]_i$ increases [6, 11]. Agents interfering specifically with calcium metabolism were efficient to regulate programmed cell death. Calcium channel blockers [12], the endoplasmic reticulum Ca^{2+}-ATPase inhibitor thapsigargin and analogues, calcium ionophores as ionomycin or 4BrA23187 were potent to lead several cell types to apoptosis [13, 14]. Effects of intracellular or extracellular Ca^{2+}-chelators on the inhibition of DNA fragmentation and the prolongation of cell survival has been frequently reported [15, 16]. Different theories have been proposed to define the biochemical consequences of a Ca^{2+} mobilization in apoptosis such as : (i) a signal transduction pathway to activate Ca^{2+}-dependent protein kinases and phosphatases may be driven by a transient rise of Ca^{2+} [5, 17]; (ii) the activity of DNA catabolic enzymes may be catalyzed by sustained concentrations of Ca^{2+} in the nucleus [18]; (iii) the depletion of intracellular bound-calcium stores could trigger apoptosis by disrupting intracellular structures [19]; (iv) mitochondrial changes associated with the nitric oxide generation, the cytochrome c release and the activation of caspases [20].

In contrast to the intracellular Ca^{2+} regulation and its influence on apoptosis, little is known on the intracellular homeostasis of $[Mg^{2+}]_i$ that is present in the cell at higher concentration than that of Ca^{2+} (10^{-3} M vs. 10^{-7} M). Recent studies have shown that the elevation of extracellular Mg^{2+} was accompanied by a consistent increase of intracellular $[Mg^{2+}]_i$ within 2–10 min [21]. Although magnesium is a positive modulator of nuclear endonucleases [22, 23], there has been no specific investigation on the influence of intracellular Mg^{2+} fluxes on apoptosis.

We report here on the spatial and temporal dynamic changes of $[Ca^{2+}]_i$ induced by thapsigargin in single living cells. The consequences of either transient increases of $[Ca^{2+}]_i$ or high and sustained $[Ca^{2+}]_i$ on apoptosis were determined. The effects of extracellular Mg^{2+} on both intracellular Mg^{2+} and Ca^{2+} fluxes were analysed in relation with the apoptosis rate induced by thapsigargin (TG). Experiments were carried out on the MCF7 breast carcinoma cell line. In parallel with $[Ca^{2+}]_i$ measurements performed by UV-microspectrofluorometry, this study was complemented by the quantification of fragmented nuclei.

Materials and methods

Chemicals

Indo-1/AM, 4BrA23187 calcium-ionophore, thapsigargin (TG) and BAPTA/AM were all purchased from Sigma Chemical Co. (St. Louis, MO, USA).

Cell culture

The MCF7 human breast cancer cell line was originally obtained from Dr. K.H. Cowan (NCI, Bethesda, MD). Cells ($2\ 10^4$/ml) were grown on 20 × 20 mm glass coverslips in RPMI 1640 medium supplemented with 10% SVF in the presence of 2 mM glutamine and antibiotics (penicillin 100 U/ml, streptomycin 100 µg/ml) under a humidified atmosphere of 5% CO_2-95% air at 37°C. Coverslips were coated with type I collagen to enhance the cell adhesion efficiency. Collagen, extracted from rat tails, was dissolved in a pH 5 acetic acid solution and filtered with a 0.22 µm filter to obtain a 1 mg/ml collagen solution. Ten µg/ml final concentration was layered on the glass coverslips during 3 h for polymerization. We have noted that type I collagen coating did not modify the $[Ca^{2+}]_i$ response and the apoptosis induction.

After 2 days of growth, the medium was changed. Cells were incubated when they reach the 600 cells/mm² density corresponding to a subconfluent culture.

DNA gel electrophoresis

10^6 cells were incubated at 50°C overnight in 20 µl of lysis buffer (150 mM NaCl, 10 mM EDTA, pH 8) containing 0.5 mg/ml Proteinase K and 0.5 % SDS. After an EtOH precipitation, extracted DNA was incubated during 1 h at 37°C with 0.1 mg/ml of RNase (DNAse free), prior to electrophoresis on 2% (w/v) agarose gel overnight at 24V.

Microspectrofluorometry

Fluorescence emission spectra within an isolated living cell were recorded using a UV confocal microspectrofluorometer (Dilor, Lille, France). An optical microscope (Olympus BH2) equipped with a water immersion objective lens (100X., N.A. 0.95, State Optical Institute of St. Petersburg, Russia) was used for this purpose. This objective lens was specially developed for the total transmission of UV radiation down to 300 nm. The axial chromatic aberration was corrected, so that both excitation (351 nm) and emission (400–500 nm) voxels were superposed. The thickness of the optical section was

controlled by varying the opening of a square pinhole from 50–1000 μm. The 351-nm laser line (Ar^+, 2065A model, Spectra Physics) was focused with a measured power of 0.5 μW at the sample. Fluorescence emission in the 360–560 nm range was spectrally dispersed by a diffraction grating, and was detected with an optical multichannel analyzer consisted of an air-cooled CCD detector.

The microspectrofluorometer scanning system (DILOR) also provides a line illumination innovation. Indeed, two synchronized scanning mirrors allow the excitation scanning on a line (X axis) and the projection of the fluorescence emission on a grating associated with a two dimensional detector. One dimension of the CCD detector corresponds to the emission spectra whereas the second corresponds to the x axis of the sample Then, emission spectra from the excited line were accumulated during 1 sec. So, a single horizontal line was virtually traced on a cell and spectra from each point of this line were recorded; spectral line scan images with space as first dimension (X axis) and time as second dimension have been collected [24].

Spectral frame images have been obtained in the same way with the use of a computer-controlled motorised stage which displaces the sample along the Y axis after a line acquisition is completed [21]. An (X, Y) motorized stage (Märzhäuser, model MCL-2 with increments of 0.1 μm) was coupled to a computer.

Determination of $[Ca^{2+}]_i$

Subconfluent cells on glass cover slips were washed twice and incubated in medium containing 5 μM Indo-1/AM for 30 min at 37°C [25]. Intracellular Ca^{2+} concentrations were calculated according to the following equation [25]:

$$[Ca^{2+}]_i = \beta.K_d.(R_f–R)/(R–R_b)$$

where R is the fluorescence intensity ratio of the sample at 410 and 500 nm; R_b and R_f represent the R ratios for the Indo-1 emissions respectively when bound and free of ions; β is the emission intensity ratio of the dye at 500 nm in free and bound forms; and K_d is the apparent dissociation constant.

To perform the *in situ* calibration, the intracellular Ca^{2+} had to be equilibrated with the extracellular Ca^{2+} as described by Millot *et al*. [26]. Briefly, cells were incubated with Indo-1/AM, washed and reincubated in medium without Indo-1/AM for 30 min (post-incubation). Then, cells were exposed 5 min to 2 μM antimycin in a buffer containing 20 mM Hepes, 150 mM NaCl, 5 mM KCl, 1 mM NaH_2PO_4, 1 mM $MgSO_4$. Then, ATP depleted cells were incubated 10 min in an hypotonic buffer (5 mM Hepes, 5 mM NaCl, 60 mM KCl, 0.5 mM KH_2PO_4, 2.5 mM $NaHCO_3$) supplemented with 0.001% Triton X100, 4 μM antimycin, 1 μM nigericin and 8 μM 4BrA23187 ionophore. Before microspectrofluorometric measurements, cells were reincubated in the isotonic buffer containing antimycin, nigericin and 4BrA23187 as above. Emission spectra from permeabilized cells in 1 mM EDTA and in saturated Ca^{2+} allowed to determine R_f and R_b, respectively.

To determine the (β.Kd) constant, emission spectra have been recorded from 25 cells in various controlled $[Ca^{2+}]_i$ such as 80, 200, 500 and 2000 nM. The linear regression line between the observed $\log(R_f–R)/(R–R_b)$ and the controlled $\log([Ca^{2+}]_i)$ has been calculated with a slope equal to 1. Then, log (β.Kd) is the x-intercept of this regression line. The (β.Kd) result was found to be 230 ± 60 and 253 ± 5 nM respectively in permeabilized cells and in buffered solution (pH 7.1). This determination of intracellular calibration constants with the Indo-1/AM probe accounts for the hydrolysis of Indo-1/AM to Indo-1 [26].

Determination of $[Mg^{2+}]_i$

For $[Mg^{2+}]_i$ analysis, cells were incubated in this medium containing the acetoxymethylester (AM) form of the magnesium sensitive dye Mag-Indo-1/AM (2 μM) for 45 min at 37°C. Cells were washed free of dye and a post-incubation was performed during 30 min to complete the hydrolysis of the dye. Under a 350 nm excitation (UV Ar^+ laser Spectra Physics, Model 2065A), fluorescence emission spectra from a living cell were recorded using a UV confocal microspectrofluorometer (DILOR, Lille, France). These emission spectra were characterized by the ratio (R) of emission intensities at 410 and 500 nm. $[Mg^{2+}]_i$ concentrations were determined according to the following equation:

$$[Mg^{2+}]_i = \beta.Kd.(R–Rmin)/(Rmax–R)$$

where β = 2.57 corresponds to the emission intensity ratio of Mag-Indo-1 emissions in saturated and free of Mg^{2+} conditions; Kd = 2.6 mM is the dissociation constant of Mag-Indo-1 for Mg^{2+}; Rmax = 0.95 and Rmin = 0.24 are the ratios of Mag-Indo-1 emissions in saturated and free of $[Mg^{2+}]_i$, respectively [21].

Staining with the DNA-binding fluorophore Hoechst 33258.

For the nucleus visualization, MCF7 living cells were stained in non-fluorescent RPMI with the DNA intercalating dye Hoechst 33258 (0.2 μg/ml for 10 min at 37°C), which present a high stability under UV excitation [27]. Fluorescence was visualized using an inverted Olympus microscope. Staining with either Indo-I or Hoechst 33258 were performed independently, due to the spectral overlap of both dyes.

Results

Dynamic changes of $[Ca^{2+}]_i$

Thapsigargin (TG) mimics the action of a variety of natural hormones and agonists by inducing the release of Ca^{2+} from intracellular stores and a consecutive Ca^{2+} influx across the plasma membrane. Laser scanning microspectrofluorometry allows to compare temporal variations of $[Ca^{2+}]_i$ between the nucleoplasm and the cytosol. Line scan dynamics were monitored to display changes of $[Ca^{2+}]_i$ along a virtual line through a single MCF7 cell after 1 μM TG addition (Fig. 1). An initial $[Ca^{2+}]_i$ of 90 ± 20 and 105 ± 30 nM was displayed in the nucleoplasm and in the cytoplasm, respectively. The exposure to TG resulted in a instant increase in $[Ca^{2+}]_i$ in the whole cell as a Ca^{2+} wave, up to 160 ± 20 nM in the nucleus and 170 ± 30 nM in the cytoplasm. This $[Ca^{2+}]_i$ rise occurred during a 100-sec time period and was followed by a smooth decay back to the initial value.

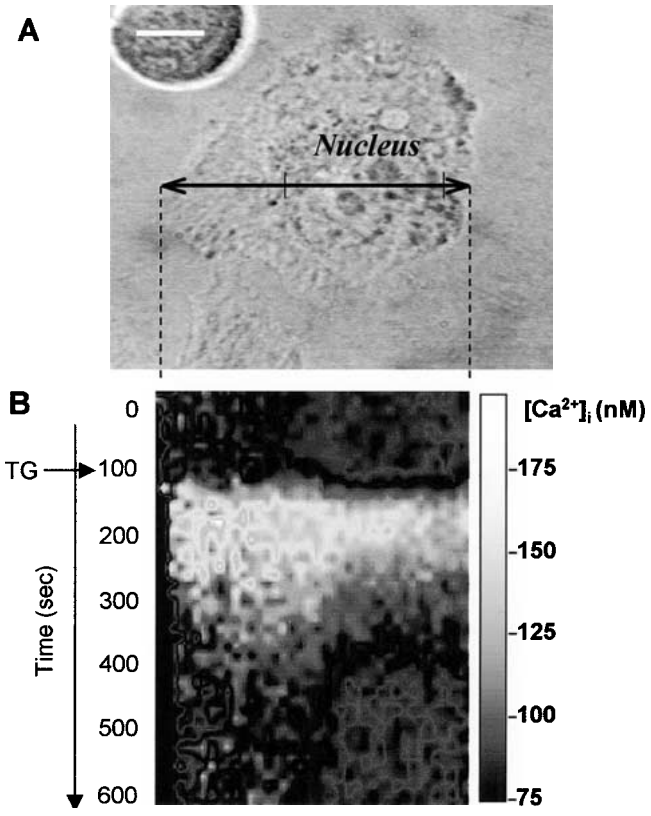

Fig. 1. (A) Videomicroscopy of an analyzed MCF7 cell. (B) Line scan image of $[Ca^{2+}]_i$ following the addition (arrow) of 1 μM thapsigargin. Analyzed segment: ↔. Bar = 5 μm.

The intracellular distribution of $[Ca^{2+}]_i$ in a representative group of cells has been determined before (Fig. 2C) and 1 h after 0.1 μM TG exposure (Fig. 2D). The integrated fluorescence emission of Indo-1 showed a homogeneous distribution of this probe within and between cells (Fig. 2B). This treatment induced an high and sustained $[Ca^{2+}]_i$ (up to 250 nM) in two out of the four analysed cells. For each cell, equivalent $[Ca^{2+}]_i$ values were observed in nucleus and cytoplasm compartments.

Means of $[Ca^{2+}]_i$ dynamics induced by TG and the 4BrA-23187 ionophore are reported in Fig. 3. In opposition to the TG concentration of 1 μM, 0.1 μM TG did not induce a significant initial $[Ca^{2+}]_i$ rise (Fig. 3A). However, after 1 h time period, elevated and sustained $[Ca^{2+}]_i$ were noted after 1 μM and 0.1 μM TG treatments. The 4BrA23187 ionophore induced a rapid rise of $[Ca^{2+}]_i$ which was followed by a decrease down to stable values after a 5–10 min exposure (Fig. 3B). The initial $[Ca^{2+}]_i$ rise depends on the 4BrA23187 ionophore concentration and would correspond to the effectiveness of molecules to carry ions by a passive diffusion across cellular membranes. High 4BrA23187 concentrations (5 and 10 μM) maintained high and sustained $[Ca^{2+}]_i$ (more than 150 nM) during several hours.

Effects of the $[Ca^{2+}]_i$ increase on apoptosis

Effects of TG and 4BrA23187 on the DNA fragmentation have been investigated in MCF7 cells. Electrophoresis on agarose gel was performed after DNA extraction from treated cells. We have checked the typical DNA ladder pattern of internucleosomal fragmentation from treated MCF7 cells with 10 μM 4BrA23187 or 0.1 μM TG during 72 h. The number of apoptotic nuclei were quantified in loaded MCF7 cells with the fluorescent dye Hoechst 33258 (Table I). $[Ca^{2+}]_i$ variations were reported after 2 and 60 min to dissociate the consequences of either initial or sustained $[Ca^{2+}]_i$ increases on apoptosis. Following a 0.1 μM TG exposure, apoptotic nuclei were observed without a detectable initial $[Ca^{2+}]_i$ increase. In contrast, a 10 min exposure with 10 μM 4BrA23187, followed by washing, induced an instant $[Ca^{2+}]_i$ rise (450 nM) and a decrease to the basal $[Ca^{2+}]_i$ after 1 h. In these conditions, no apoptotic nuclei were detected (Table 1). This suggests that the early high $[Ca^{2+}]_i$ increases are not determinant in the events triggering apoptosis.

To evaluate the contribution of the high and sustained $[Ca^{2+}]_i$ on the activation of the genome degradation, cells were incubated with the intracellular chelator BAPTA for 1 h and were washed before the TG exposure. $[Ca^{2+}]_i$ of BAPTA loaded cells remained lower than control cells (Table 1). The nuclear fragmentation elicited by 0.1 μM TG was partially reduced by BAPTA, that indicates the influence of the high and sustained $[Ca^{2+}]_i$ for triggering apoptosis (Table 1).

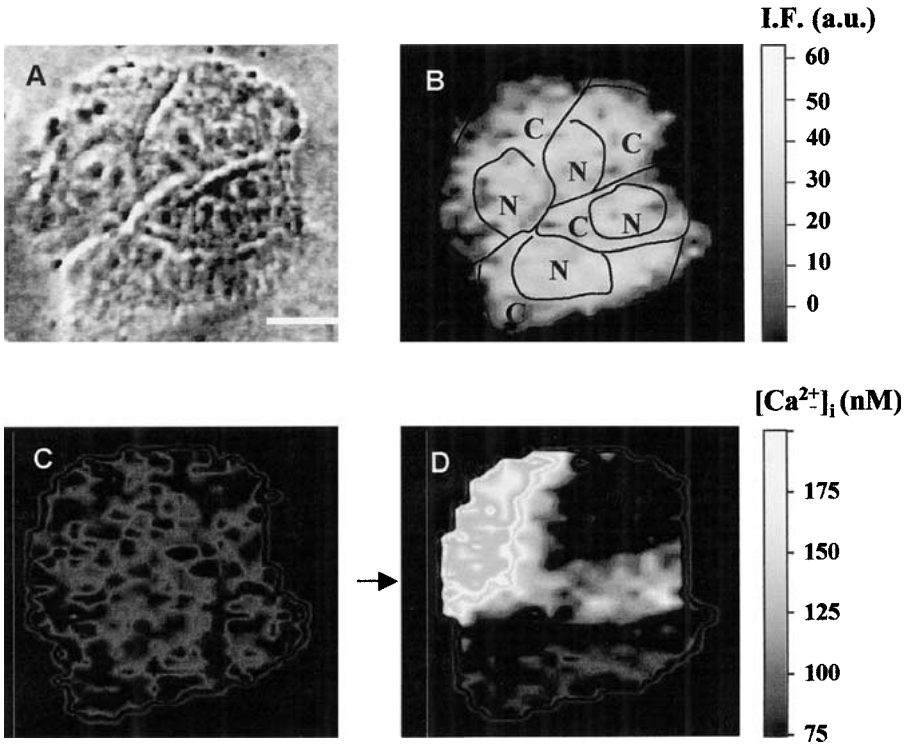

Fig. 2. (A) Videomicroscopy of MCF7 cells in monolayer culture (bar = 10 μm). (B) Integrated fluorescence intensity of Indo-1 (400–600 nm) and schematic representation of cell limits; intracellular distribution of $[Ca^{2+}]_i$ before (C) and 1 h (D) after addition of 0.1 μM thapsigargin.

Effects of extracellular Mg^{2+}

As TG induced both apoptosis and a sustained $[Ca^{2+}]_i$ increase, a possible interaction between intracellular Mg^{2+} and Ca^{2+} has been studied. First, concentrations of intracellular Mg^{2+} were determined as a function of extracellular Mg^{2+}. As shown in Fig. 4, an increase of the extracellular Mg^{2+} concentration from 1.4–10 mM caused an increase in basal $[Mg^{2+}]_i$ from 0.8 ± 0.3 to 1.6 ± 0.5 mM. This variation of $[Mg^{2+}]_i$ was less important than those of extracellular Mg^{2+} and agrees with data of our previous reports [21, 28]. In addition, since 1 μM TG did not modify the $[Mg^{2+}]_i$ influx in MCF7 cells (Fig. 4), the Mg^{2+} influx pathway does not seem to interfere with the Ca^{2+} influx pathway.

Second, the TG-mediated apoptosis has been observed for 0–10 mM extracellular Mg^{2+} (Fig. 5). After 48 h of 1 μM TG exposure, percentages of apoptotic nuclei in 10 mM extracellular Mg^{2+} were 2 fold lower than in the concentration range of 0–5 mM extracellular Mg^{2+}.

Third, the effects of extracellular Mg^{2+} on the $[Ca^{2+}]_i$ rise induced by TG were observed (Fig. 6). Experiments in a free of Ca^{2+} medium investigated the effect of extracellular Mg^{2+}

Table 1. Apoptosis and $[Ca^{2+}]_i$ increases in treated MCF7 cells

	Incubation time	Increase of $[Ca^{2+}]_i$ (nM) after 2 min § (n = 30)	Increase of $[Ca^{2+}]_i$ (nM) after 60 min § (n = 30)	Apoptotic nuclei after 48 hours (%) (n = 200)
4BrA23187 (10 μM)	10 min	450 ± 50#	NS	3 ± 3
4BrA23187 (10 μM)	Continuous	450 ± 50#	160 ± 130#	23 ± 5*
TG (0.1 μM)	Continuous	NS	70 ± 30#	22 ± 4*
TG (1 μM)	Continuous	70 ± 50#	90 ± 40#	23 ± 5*
TG (1μM) + BAPTA (a)	Continuous	–30 ± 20	–30 ± 20	10 ± 4
BAPTA (a)	Continuous	–30 ± 20	–30 ± 20	3 ± 2
Untreated cells	NS	NS	3 ± 2	3 ± 2

§ – In comparison with initial value of $[Ca^{2+}]_i$ (80 ± 15 nM); #significant increase of $[Ca^{2+}]_i$ ($p < 0.01$); NS – no significant variation of $[Ca^{2+}]_i$; *significant increase of apoptotic nuclei % after 48 h ($p < 0.01$); (a) – Cells were incubated for 1 h with 25 μM BAPTA and washed before 48 h TG exposure.

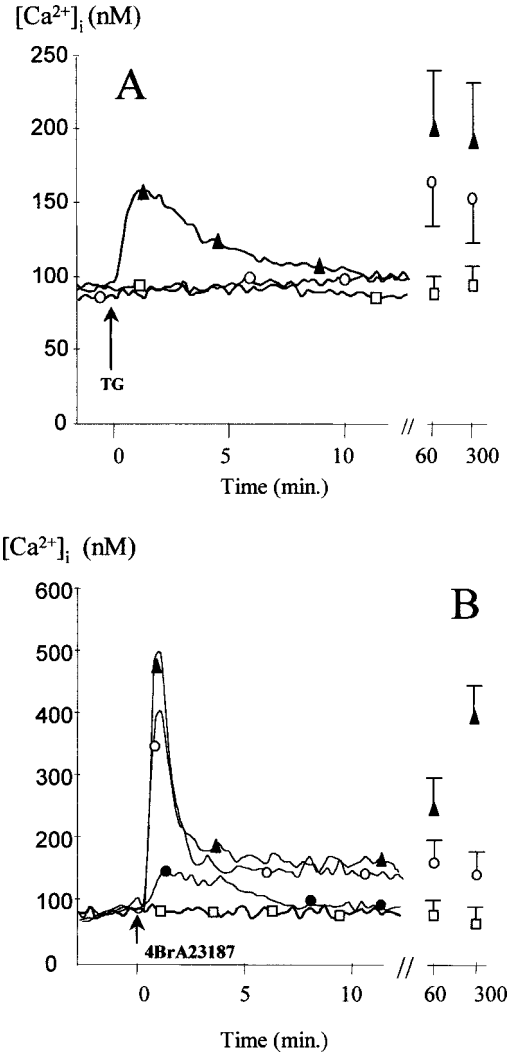

Fig. 3. (A) Means of dynamic changes of $[Ca^{2+}]_i$ in MCF7 cells (n = 5) after addition of thapsigargin (▲ – 1 μM; O – 0.1 μM; □ – control cells). (B) Means of dynamic changes of $[Ca^{2+}]_i$ in MCF7 cells (n = 5) after addition of 4BrA23187 calcium ionophore (▲ – 10 μM; O – 5 μM; ● – 1.25 μM; □ – control cells).

on the Ca^{2+} discharge from intracellular calcium stores. In the absence of extracellular Ca^{2+}, extracellular Mg^{2+} did not modulate on the $[Ca^{2+}]_i$ response to TG which corresponds to the Ca^{2+} release from intracellular stores. In presence of 2 mM extracellular Ca^{2+}, the $[Ca^{2+}]_i$ increase reflected both the Ca^{2+} depletion of the endoplasmic reticulum and the consecutive Ca^{2+} influx through the plasma membrane. For 1.4 and 10 mM Mg^{2+}, initial $[Ca^{2+}]_I$ rises were equivalent. These increases were followed by a faster decay back to the baseline for 10 mM than for 1.4 mM extracellular Mg^{2+}. This suggests a partial inhibition of the Ca^{2+} influx through the plasma membrane in the presence of high extracellular Mg^{2+}. After 5 h of TG exposure, $[Ca^{2+}]_i$ was significantly lower in 10 mM

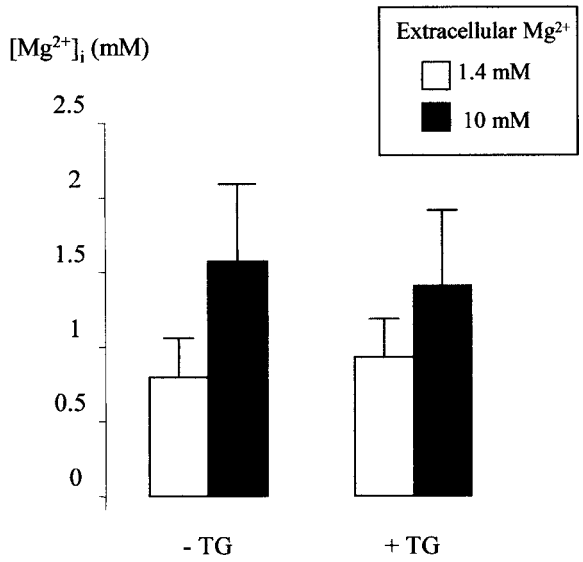

Fig. 4. Effect of extracellular Mg^{2+} (□ – 1.4 mM; ■ – 10 mM) on $[Mg^{2+}]_i$ in untreated cells and in 1 μM thapsigargin treated cells during 1 h. Each points represents the mean ± S.E. of 3 independent determinations from 15 different isolated cells.

($[Ca^{2+}]_i$ = 132 ± 20 nM) than in 1.4 mM extracellular Mg^{2+} ($[Ca^{2+}]_i$ = 172 ± 23 nM), showing that the high and sustained $[Ca^{2+}]_i$ increase was modulated by high extracellular Mg^{2+} (Fig. 6).

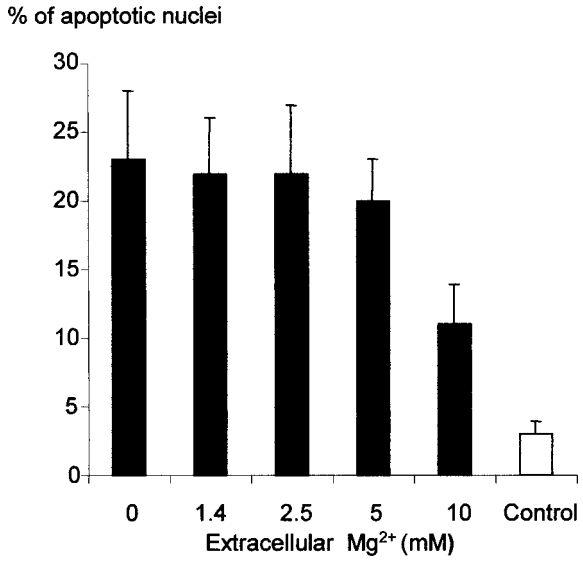

Fig. 5. Effect of extracellular Mg^{2+} on the thapsigargin-induced apoptosis. MCF7 cells are treated in presence of 1 μM thapsigargin and apoptotic nuclei are determined after 48 h (n = 600).

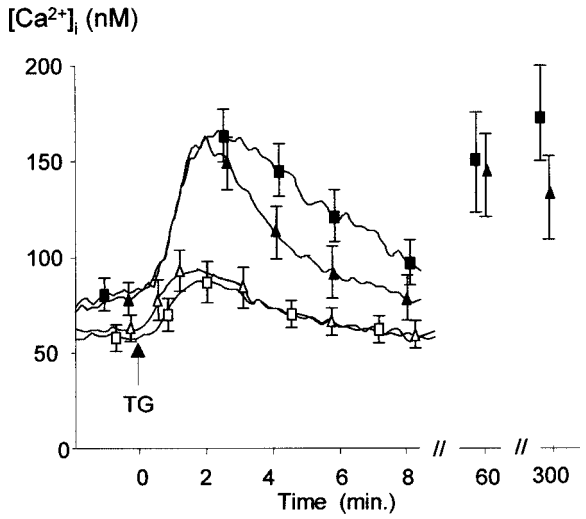

Fig. 6. Effect of extracellular Mg^{2+} and Ca^{2+} on the $[Ca^{2+}]_i$ changes after 1 μM thapsigargin addition. In 2 mM extracellular Ca^{2+}: ▲ – 10 mM of extracellular Mg^{2+}; ■ – 1.4 mM of extracellular Mg^{2+}; In free of extracellular Ca^{2+}: Δ – 10 mM of extracellular Mg^{2+}; □ – 1.4 mM of extracellular Mg^{2+}. Each point represents the mean ± S.E. of 3 independent determinations from 15 different isolated cells.

Discussion

The concept that $[Ca^{2+}]_i$ increases can initiate apoptosis has been suggested when rises in $[Ca^{2+}]_i$ have been observed prior to the genome fragmentation and cell death. Several studies have shown transient changes in $[Ca^{2+}]_i$ following agents – or radiations – which induced apoptosis, suggesting initial Ca^{2+} influx as a prominent stimulus for apoptosis [6]. The microsomal Ca^{2+}-ATPase inhibitor thapsigargin and the 4BrA23187 calcium-ionophore are known to stimulate both dynamic changes in intracellular calcium and apoptosis in several cell types. Thus, in this study, MCF7 cells were treated with these agents to determine whether apoptosis can be initiated by either transient or sustained alterations in calcium homeostasis.

Increases of $[Ca^{2+}]_i$ elicited by thapsigargin were similar to those observed during ionic channels stimulation and mimic a Ca^{2+}-dependent physiological mechanism. Although thapsigargin acts specifically on the reticular Ca^{2+}-ATPase pump [29, 30], it has been demonstrated that the rise in $[Ca^{2+}]_i$, induced by this blocker was enhanced by a calcium influx throughout the plasma membrane. This process, termed capacitative calcium entry [31, 32] could involve a small diffusing messenger, named Calcium Influx Factor (CIF) in GTP dependent mechanisms [33]. The thapsigargin treatment resulted in an early rise just after the blocker addition and a progressive increase later. This Ca^{2+} influx was observed not only in the cytosol but also in the nucleus as a calcium wave throughout the cell, which was dependent on the TG concentration. After several hours of thapsigargin exposure, high levels of $[Ca^{2+}]_i$ were observed in all compartments, suggesting a deregulation of the calcium homeostasis. Thus, biochemical modifications such as the activation of calcium-dependent enzymes may appear in the nuclear compartment before the genome fragmentation.

Our results show that the thapsigargin- and ionophore-induced apoptosis is associated with elevated and sustained $[Ca^{2+}]_i$ but not with the early rise of $[Ca^{2+}]_i$. Indeed, when MCF7 cells have been washed extensively just after the initial $[Ca^{2+}]_i$ rise induced by high doses of 4BrA23187, no apoptosis was detected. Besides, the apoptosis triggered by 0.1 μM TG was preceded by a high $[Ca^{2+}]_i$ during several hours but not by the early $[Ca^{2+}]_i$ increase. A threshold of $[Ca^{2+}]_i$ must be reached and maintained over a critical period to initiate apoptosis. Similar results have been observed in prostatic cancer cells [34] and in thymocytes [35] undergoing programmed cell death. Maintained and elevated $[Ca^{2+}]_i$ over a critical period have been also noted in human hepatoma cells during the programmed cell death induced by thapsigargin [36].

Direct evidences that $[Ca^{2+}]_i$ increases are important for apoptosis have been obtained from experiments with intracellular Ca^{2+}-chelators (Quin-2, BAPTA). These agents can inhibit $[Ca^{2+}]_i$ increases, DNA fragmentation and cell death induced by glucocorticoids [15] or tamoxifene [37]. Moreover, transfected cells with the avian calbindin D Ca^{2+} buffering protein have shown that a thapsigargin-induced apoptosis was dependent of a sustained elevation in $[Ca^{2+}]_i$ and not of the depletion of the endoplasmic reticulum pools of Ca^{2+} [38]. In our study, the inhibition of the sustained $[Ca^{2+}]_i$ increase by BAPTA modulates partially the number of apoptotic nuclei, suggesting that apoptosis is not totally dependent of $[Ca^{2+}]_i$.

In contrast to the well studied role of Ca^{2+}, little is known about the intracellular regulation of Mg in proliferating cells, differentiated cells and cells in apoptosis. $[Mg^{2+}]_i$ has been determined as 0.8 mM in our study. The rise of extracellular Mg^{2+} from 1.4–10 mM, allows the increase of $[Mg^{2+}]_i$ from 0.8–1.6 mM. The $[Mg^{2+}]_i$ did not reach the extracellular Mg^{2+} concentration, confirming the presence of regulation mechanisms to maintain $[Mg^{2+}]_i$ in a physiological range. It has been reported that the Mg^{2+} influx through the plasma membrane shows similar characteristics to voltage-gate Ca^{2+} channels [39].

Effects of extracellular Mg^{2+} on $[Ca^{2+}]_i$ after an agonist stimulation was delineated. We clearly show that extracellular Mg^{2+} modulates both the TG-stimulated $[Ca^{2+}]_i$ rise and the induced apoptosis. In a medium free of Ca^{2+}, extracellular Mg^{2+} does not modulate the discharge of intracellular calcium stores induced by thapsigargin. Extracellular Mg^{2+} appears mainly to modulate the store-dependent capacitative Ca^{2+} influx. We have also reported on human tracheal secre-

tory gland cells that extracellular Mg reduced the influx of extracellular Ca^{2+} stimulated by histamine [21]. In vascular smooth muscle cells, it has been described that the contraction and $[Ca^{2+}]_i$ changes induced by TG are modulated by extracellular Mg^{2+} [40]. To account for this modulation role of Mg^{2+}, it has been suggested that extracellular Mg^{2+} would limit the capacitative Ca^{2+} entry [41].

A complex equilibrium among compartments and between the bound and free forms of Mg would contribute to the concentration of free cytosolic Mg^{2+} [42]. About 98–99% of total intracellular Mg and 94% of cytosolic Mg are complexed to nucleic acids, proteins or membranes [43]. For an understanding of intracellular magnesium homeostasis and its regulation, measurements of total intracellular magnesium could be performed, in addition to the analysis of the free cytosolic form. Total magnesium can be analysed by atomic absorption spectrophotometry [44]. Electron probe X-ray microanalysis has been also applied to determine the total Mg at the subcellular level. In UV light-irradiated U937 apoptotic cells, no difference of total Mg occurred before and after the induction of apoptosis [45].

In conclusion, high extracellular Mg^{2+} inhibits TG-induced cytosolic Ca^{2+} influx and the consecutive apoptosis. Apoptotic nuclei are observed in MCF7 cells when elevated and sustained $[Ca^{2+}]_i$ are maintained in the nucleus for several hours.

Acknowledgement

The authors are grateful to G.D. Sockalingum for revision of the manuscript.

References

1. Kerr JFR, Wyllie AH, Currie AR: Apoptosis: A basic biological phenomenon with wide ranging implications in tissue kinetics. Br J Cancer 26: 239–257, 1972
2. Wyllie AH, Rose KA, Morris RG, Steel CM, Forster E, Spandidos DA: Rodent fibroblast tumours expressing human myc and ras genes: Growth, metastasis and endogeous oncogene expression. Br J Cancer 56: 251–259, 1987
3. Raff MC, Barres BA, Burne JF, Coles HS, Ishizaki Y, Jacobson MD: Programmed cell death and the control of cell survival: Lessons from the nervous system. Science 262: 695–700, 1993
4. Williams GT: Apoptosis in the immune system. J Pathol 173: 1–4, 1994
5. McConkey DJ, Hartzell P, Amador-Perez JF, Orrenius S, Jondal M: Calcium-dependent killing of immature thymocytes by stimulation via the CD3/T cell receptor complex. J Immunol 143: 1801–1806, 1989
6. Bodey B, Bodey B Jr, Kaiser HE: Apoptosis in the mammalian thymus during normal histogenesis and under various *in vitro* and *in vivo* experimental conditions. *In Vivo* 12: 123–133, 1998
7. Cohen JJ, Duke RC: Glucocorticoid activation of a calcium-dependent endonuclease in thymocytes nuclei leads to cell death. J Immunol 132: 38–42, 1984
8. Ribeiro JM, Carson DA: Ca^{2+}/Mg^{2+}-dependent endonuclease from human spleen: Purification, properties, and role in apoptosis. Biochemistry 32: 9129–9136, 1993
9. Bellomo G, Perotti M, Mirabelli F, Finardi G, Nicoreta P, Orrenius S: Tumor necrosis α induces apoptosis in mammary adenocarcinoma cells by an increase in intranuclear free Ca^{2+} concentration and DNA fragmentation. Cancer Res 52: 1342–1346, 1992
10. Gupta PD, Pushkala K: Importance of the role of calcium in programmed cell death: a review. Cytobios 99: 83–95, 1999
11. Todd DG, Mikkelsen RB: Ionizing radiations induces a transient increase in cytosolic free $[Ca^{2+}]$ in human epithelial tumor cells. Cancer Res 54: 5224–5230, 1994
12. Balakuraman A, Campbell GA, Molsen MT: Calcium channel blockers induce thymic apoptosis *in vivo* in rats. Toxicol Appl Pharmacol 139: 122–127, 1996
13. Christensen SB, Andersen A, Kromann H, Treiman M, Tombal B, Denmeade S, Isaacs JT: Thapsigargin analogues for targeting programmed death of androgen-independent prostate cancer cells. Bioorg Med Chem 7: 1273–1280, 1999
14. Martikainen P, Kyprianou N, Tucker RW, Isaacs JT: Programmed death of nonproliferating androgen-independent prostatic cancer cells. Cancer Res 51: 4693–4700, 1991
15. Zhivotovsky B, Cederval B, Jiang S, Nicoreta P, Orrenius S: Involvement of Ca^{2+} in the formation of high molecular weight DNA fragments in thymocytes apoptosis. Biochem Biophys Res Comm 202: 120–127, 1994
16. Lin XS, Denmeade SR, Cisek L, Isaacs JT: Mechanism and role of growth arrest in programmed (apoptotic) death of prostatic cancer cells induced by thapsigargin. Prostate 33: 201–207, 1997
17. Shan D, Ledbetter JA, Press OW: Signaling events involved in anti-CD20-induced apoptosis of malignant human B cells. Cancer Immunol Immunother 48: 673–683, 2000
18. Khodarev NN, Ashwell JD: An inducible lymphocyte nuclear Ca^{2+}/Mg^{2+}-dependent endonuclease associated with apoptosis. J Immunol 156: 922–931, 1996
19. Reynolds JE, Eastman A: Intracellular calcium stores are not required for Bcl-2-mediated protection from apoptosis. J Biol Chem 271: 27739–27743, 1996
20. Srivastava RK, Sollott SJ, Khan L, Hansford R, Lakatta EG, Longo DL: Bcl-2 and Bcl X(L) block thapsigargin-induced nitric oxide generation, c-Jun NH(2)-terminal kinase activity, and apoptosis. Mol Cell Biol 19: 5659–5674, 1999
21. Sebille S, Millot JM, Maizières M, Arnaud M, Delabroise AM, Jacquot J, Manfait M: Spatial and temporal Mg^{2+} signaling in single human tracheal gland cells. Biochem Biophys Res Commun 227: 743–749, 1996
22. Robertson JD, Orrenius S, Zhivotovsky B: Review: Nuclear events in apoptosis. J Struct Biol 129: 346–358, 2000
23. Yakovlev AG, Wang G, Stoica BA, Boulares HA, Spoonde AY, Yoshihara K, Smulson ME: A role of the Ca^{2+}/Mg^{2+}-dependent endonuclease in apoptosis and its inhibition by Poly(ADP-ribose) polymerase. J Biol Chem 275: 21302–21308, 2000
24. Jacquot J, Maizières M, Spilmont C, Millot JM, Sebille S, Merten M, Kammouni W, Manfait M: Intracellular free Ca^{2+} dynamic changes to histamine are reduced in cystic fibrosis human tracheal gland cells. FEBS Lett 386: 123–127, 1996
25. Grynkiewicz G, Poenie M, Tsien RY: A new generation of Ca^{2+} indicators with greatly improved fluorescence properties. J Biol Chem 260: 3440–3450, 1985
26. Millot JM, Pingret L, Angiboust JF, Bonhomme A, Pinon JM, Manfait M: Quantitative determination of free calcium in subcellular compartments, as probed by Indo-1 and confocal microspectrofluorometry. Cell Calcium 17: 354–366, 1995
27. Elstein KH, Zucker RM: Comparison of cellular and nuclear flow cytometric techniques discriminating apoptotic subpopulations. Exp Cell Res 211: 322–331, 1994

28. Sebille S, Pereira M, Millot JM, Jacquot J, Delabroise AM, Arnaud M, Manfait M: Extracellular Mg^{2+} inhibits both histamine-stimulated Ca^{2+}-signaling and exocytosis in human tracheal secretory gland cells. Biochem Biophys Res Comm 246: 111–116, 1998
29. Thastrup O, Dawson AP, Scharff O, Foder B, Cullen PJ, Drobak BK, Bjerrum PJ, Christensen SB, Hanley MR: Thapsigargin, a novel molecular probe for studying intracellular calcium release and storage. Agents Action 27: 17–23, 1989
30. Waldron RT, Short AD, Meadows JJ, Ghosh TK, Gill DL: Endoplasmic reticulum calcium pump expression and control of cell growth. J Biol Chem 269: 11927–11933, 1994
31. Putney JW, Bird GJ: The signal for capacitative calcium entry. Cell 75: 199–201, 1993
32. Rossato M, Bordon P, Di Virgilio F, Foresta C: Capacitative calcium entry in rat Sertoli cells. J Endocrinol Invest 19: 516–523, 1996
33. Artalejo AR, Ellory JC, Parekh AB: Ca^{2+}-dependent capacitance increases in rat basophilic leukemia cells following activation of store-operated Ca^{2+} entry and dialysis with high-Ca^{2+}-containing intracellular solution. Pflügers Arch 436: 934–939, 1998
34. Tombal B, Weeraratna AT, Denmeade SR, Isaacs JT: Thapsigargin induces a calmodulin/calcineurin-dependent apoptotic cascade responsible for the death of prostatic cancer cells. Prostate 43: 303–317, 2000
35. Jiang S, Chow SC, Nicoreta P, Orrenius S: Intracellular Ca^{2+} signals activate apoptosis in thymocytes: Studies using the Ca^{2+}-ATPase inhibitor thapsigargin. Exp Cell Res 212: 84–92, 1994
36. Kaneko Y, Tsukamoto A: Thapsigargin-induced persistent intracellular calcium pool depletion and apoptosis in human hepatoma cells. Cancer Lett 79: 147–155, 1994
37. Kim JA, Kang YS, Jung MW, Lee SH, Lee YS: Involvement of Ca^{2+} influx in the mechanism of tamoxifen-induced apoptosis in HepG2 human hepatoblastoma cells. Cancer Lett 147: 115–123, 1999
38. Furuya Y, Lundmo P, Short AD, Gill DL, Isaacs JT: The role of calcium, pH, and cell proliferation in the programmed (apoptotic) death of androgen-independent prostatic cancer cells induced by thapsigargin. Cancer Res 54: 6167–6175, 1994
39. Quamme GA, Dai LJ, Rabkin SW: Dynamics of intracellular free Mg^{2+} changes in a vascular smooth muscle cell line. Am J Physiol 265: H281–H288, 1993
40. Zhu Z, Tepel M, Spieker C, Zidek W: Effect of extracellular Mg^{2+} concentration on agonist-induced cytosolic free Ca^{2+} transients. Biochim Biophys Acta 1265: 89–92, 1995
41. Yoshimura M, Oshima T, Matsuura H, Ishida T, Kambe M, Kajiyama G: Extracellular Mg^{2+} inhibits capacitative Ca^{2+} entry in vascular smooth muscle cells. Circulation 95: 2567–2572, 1997
42. Cittadini A, Wolf FI, Bossi D, Calviello G: Magnesium in normal and neoplastic cell proliferation: State of the art on *in vitro* data. Magnes Res 4: 23–33, 1991
43. Corkey BE, Duszynski J, Rich TL, Matschinsky B, Williamson JR: Regulation of free and bound magnesium in rat hepatocytes and isolated mitochondria. J Biol Chem 261: 2567–2574, 1986
44. Yago MD, Manas M, Singh J : Intracellular magnesium : Transport and regulation in epithelial secretory cells. Frontiers in Biosci 5: d602–d618, 2000
45. Fernandez-Segura E, Canizares FJ, Cubero MA, Warley A, Campos A: Changes in elemental content during apoptotic cell death studied by electron probe X-ray microanalysis. Exp Cell Res 253: 454–462, 1999